Empowering the Tracking Performance of LEO PNT by Means of Meta-Signals

Empowering the Tracking Performance of LEO PNT by Means of Meta-Signals

Andrea Nardin*, Fabio Dovis*, Juan A. Fraire†‡
*Departement of Electronics and Telecommunications, Politecnico di Torino, Turin, Italy
†CONICET - Universidad Nacional de Córdoba, Córdoba, Argentina
‡Saarland University, Saarland Informatics Campus, Saarbrücken, Germany

***Abstract*—Global Navigation Satellite Systems (GNSSs) are by far the most widespread technology for Position Navigation and Timing (PNT). They have been traditionally deployed exploiting Medium Earth Orbit (MEO) or Geostationary Earth Orbit (GEO) satellite constellations. To meet future demands and overcome MEO and GEO limitations, GNSSs based on Low Earth Orbit (LEO) constellations have been investigated as a radical system change. Although characterized by a higher Doppler effect, a PNT service supplied by means of LEO satellites can provide received signals that are about 30 dB stronger. Moreover, existing LEO constellations and the forthcoming mega-constellations, which are designed for broadband internet coverage, can be exploited to provide a piggybacked PNT service. With this cost-effective solution, a secondary PNT service might be subject to an economical use of resources, which may result in substantial bandwidth limitations. At the same time, the introduction of meta-signals in the GNSS literature has brought a new receiver signal processing strategy, particularly effective in terms of available bandwidth exploitation. It allows to increase the positioning accuracy exploiting a wideband processing approach, which might be challenging under severe Doppler conditions. A narrowband implementation of the meta-signal concept, namely Virtual Wideband (VWB) can tolerate harsh Doppler conditions while also reducing the processed bandwidth. It is thus more effective when addressing a secondary PNT service, where a limited frequency occupation might be an essential requirement. The aim of this work is to show the applicability of a VWB receiver architecture on signals provided by a piggybacked PNT service, hosted on a broadband LEO constellation. We demonstrate the capability of this implementation to bear high Doppler conditions while empowering the potential of LEO PNT.**

***Index Terms*—Amazon Kuiper, DLL, GNSS , LEO PNT, mega-constellations, meta-signals, tracking**

I. Introduction

Global Navigation Satellite Systems (GNSSs) are by far the most widespread technology for Position Navigation and Timing (PNT). They have been traditionally deployed exploiting Medium Earth Orbit (MEO) or Geostationary Earth Orbit (GEO) satellite constellations. However, upcoming PNT applications are going to have challenging requirements and a radical system change might be needed to satisfy those demands.

Global macro-trends are going to drive the use of GNSS by industries and individuals demanding higher PNT accuracy and security [1]. However, signals' low power and limited bandwidth are intrinsic characteristics of current GNSSs that bound the achievable accuracy and threaten the robustness to intentional (jamming) and unintentional interference [2]. MEO and GEO GNSS signals are indeed subject to a strong free-space loss due to their long distance from Earth and they are all transmitted in the overcrowded L band, where bandwidth availability is scarce [2].

To meet future demands and overcome limitations, GNSSs based on Low Earth Orbit (LEO) constellations have been investigated as a radical system change. Although operating in a high Doppler effect scenario, a PNT service based on LEO satellites would offer a 30 dB smaller zenith path loss w.r.t. transmissions from MEO satellites [3]. Proposals for dedicated LEO GNSS constellations exist [3], but a promising approach relies on exploiting global internet broadband constellations for PNT services [4]–[6]. The Iridium constellation is already providing a *hosted* PNT service [6] and new possibilities are foreseen thanks to companies like Amazon, Telesat and SpaceX, which are deploying the so-called *mega-constellations* to provide global broadband internet [3].

The potential of a hosted PNT payload on LEO constellations has been analyzed in [4], [5] addressing dedicated PNT hardware on board. One step further is the *fused* approach, where existing broadband service resources (e.g. clocks, antennas, spectrum) are simultaneously exploited for PNT, providing a cost effective solution without reducing performance [7]. Major players for broadband mega-constellations are planning to transmit over sparsely occupied frequency bands (Ka, Ku, K, V bands) [3], potentially favoring a larger PNT-dedicated bandwidth w.r.t. traditional L-band GNSS. However, despite the bandwidth availability, a fused solution will be subject to resource limitations that depend on its commercial value with respect to the primary service and spectral resources are no exception.

High Doppler and an economical use of bandwidth are not the only drawbacks of fused LEO PNT solutions. Although there are potentially many satellites flying by simultaneously over a single spot, LEO broadband constellations are mainly designed to have only one satellite serving a cell at any given time. Nonetheless the radio visibility of only a single PNT signal essentially prevents single-epoch pseudorange positioning. A strategy to overcome this problem is provided in [7]. According to the authors, PNT bursts can be directed towards neighboring cells for a fraction of the downlink communication time, causing a commercial loss, whose sustainability can be calculated.

The introduction of *meta-signals* in the GNSS literature [8], [9] has brought a new receiver signal processing strategy, which is particularly effective in terms of available bandwidth exploitation. It allows to increase the positioning accuracy of a set of PNT signals, taking advantage of their frequency separation [10]. However, a wideband processing strategy might be critical when signals are affected by severe Doppler since a wideband signal is interested by a broader range of Doppler frequency shifts.

A more flexible implementation of the meta-signal concept has been presented in [11], overcoming the constrained distance between carrier frequencies. This approach leverages meta-signals by jointly processing PNT narrowband signals that may even share the same bandwidth, thus building a *Virtual Wideband* (VWB) signal. A VWB processing strategy is more effective when addressing a secondary PNT service, where a severely limited band occupation might be an essential requirement. Moreover it can tolerate harsh Doppler conditions thanks to its narrowband implementation.

The aim of this work is to show the applicability of a VWB meta-signal receiver architecture on signals provided through a fused LEO PNT service. We demonstrate the capability of this implementation to bear high Doppler conditions while empowering the potential of LEO PNT. Amazon's mega-constellation project Kuiper [12] is taken here as a sample candidate for a hypothetical fused LEO PNT service, by relying on the technical data in [13]. Thanks to a Software Defined Network (SDN) approach, the high level of flexibility provided by its payload [13] makes it a good candidate for a fused service. The initial service constellation has been simulated along with atmospheric conditions to extract realistic Doppler profiles and C/N_0 values for three reference locations on Earth (low, intermediate and high Doppler conditions). A signal generator has been used to generate two BPSK-modulated LEO PNT signals consistent with the simulated Doppler characteristics and C/N_0 values. The signals are then jointly processed in a VWB fashion through a GNSS software receiver.

Section II will introduce the meta-signals and the VWB approach. The satellite data acquisition and the signal generation process are described in detail in Section III along with the software receiver implementation. Results are then discussed in Section IV and conclusions are drawn in Section V.

II. The Meta-signal concept

The meta-signal processing (MSP) approach introduced in [8] is based on the well-known relationship between the Gabor Bandwidth (GB) and the Cramér-Rao Lower Bound of the code thermal noise in a Delay-locked Loop (DLL) [2]:

$$\sigma^2_{DLL,CRLB} = \frac{B_n}{C/N_0 4\pi^2 \int_{-\infty}^{+\infty} f^2 G_s(f) df} \,. \tag{1}$$

In (1) B_n is the DLL bandwidth and C/N_0 and G_s are respectively the carrier-to-noise-density ratio and the normalized power spectral density of the processed signal. The term

$$B_{GB} = \sqrt{\int_{-\infty}^{+\infty} f^2 G_s(f) df} \tag{2}$$

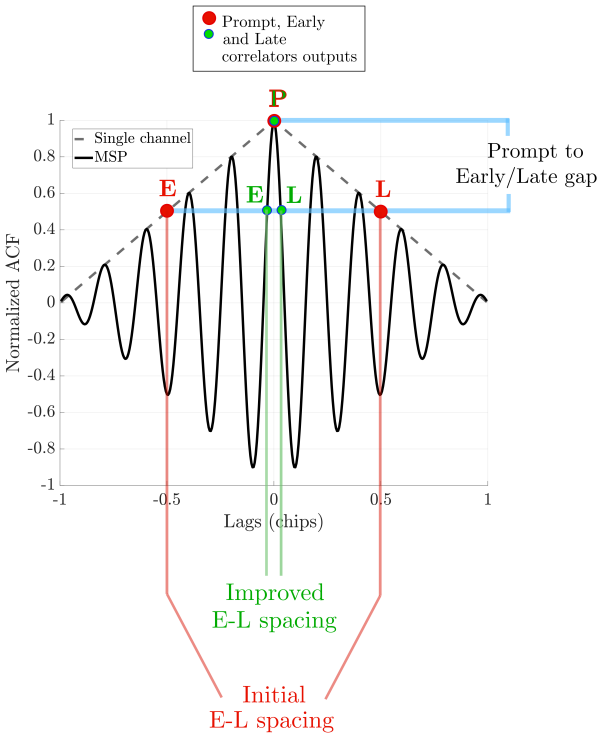

Fig. 1: Autocorrelation function of a single BPSK signal and a meta-signal made by two BPSK channels.

is indeed the GB and it is directly related to the code delay estimation precision as they both increase according to (1).

This concept motivated the definition of a wideband processing strategy that aims at maximizing the GB of the processed signal by jointly tracking two frequency-separated PNT channels as a single wideband channel [9]. The channels are thus at the edges of the power spectral density of the processed signal, resulting in an increased GB. The net result is a superposition of the frequency-shifted versions of the original channels, which is processed within the baseband DSP chain. By looking it from a different perspective, this "meta-signal" presents an Auto-correlation Function (ACF) which is essentially modulated by a complex exponential [9]. As reported in Figure 1, such an ACF has a narrower main peak, a property directly related to a code tracking performance improvement [14]. The ACF exhibits also an increased peak ambiguity, whose severeness depends on the frequency separation between the combined channels. Therefore, as long as we are able to tolerate the ambiguity, it is possible to exploit the increased sharpness to reduce the correlator Early-minus-Late (E-L) spacing, while keeping the gap between Prompt (P) and Early (E) or Late (L) correlator outputs constant (see Figure 1). This means that we can tolerate the same amount of noise (thanks to the gap) while attaining an improved code tracking jitter (thanks to E-L spacing reduction) [15].

An additional approach to MSP has been introduced in [11]. According to this architecture, two narrowband signals are received by a front-end stage and fed to the processing chain

as baseband signals. Within the tracking loop, these signals are up-converted to two opposite frequencies, thus introducing a frequency separation between them. The signals are then correlated with local replicas and combined at a post-correlator level. Through this method an equivalent VWB signal is processed in the receiver at the cost of a complexity increase. Nonetheless, the resulting flexibility overcomes two major limitations of standard MSP. First, the separate narrowband band processing of the two PNT channels enables a two-stages peak ambiguity resolution scheme. The narrowband channels are processed independently, in a standard *single-channel* processing, to solve the peak ambiguity. The MSP phase is then triggered only once the receiver is locked over the main peak. Referring again to Figure 1, by processing a single BPSK channel we are able to align the DLL consistently with the dashed grey ACF in the diagram. If the main peak of this curve is estimated with sufficiently high precision, the receiver is able to lock over the main peak of the meta-signal's ACF. The ambiguity is solved by means of the narrowband signals while the improved accuracy is brought by the VWB blocks, similarly to a fixed-tone ranging system [11], [16]. The second advantage of this flexible architecture is that it allows to adjust the frequency separation of the channels within the DSP chain. It is then possible to further enhance the GB for channels that have a small or even null frequency separation in the Signal-In-Space. This might be a substantial advantage in the LEO PNT framework, where a small carrier frequency difference results in a significant variation of Doppler frequency shift.

III. Signal Generation and processing

In this Section we describe the data collection process that led to the PNT signals generation. Doppler shift profiles and power levels extracted from the constellation simulator have been fed to the binary signal generator to simulate the received PNT signals. A description of the receiver configuration employed to track those signals is also provided.

A. Reference Constellation Scenario

In order to analyze the applicability of VWB PNT in upcoming mega-constellations, we consider, as a case-study, the Amazon's mega-constellation project Kuiper. According to [13], Kuiper fleet will be composed of 3236 LEO satellites providing high-speed and low-latency satellite broadband services. Satellites will be deployed in three "shells" at different altitudes, over circular orbits (see Table I). In this work, we consider the plane at 630 km height, the first to be deployed, as indicated in [13]. On the ground segment side, the network will leverage existing Amazon's terrestrial networking infrastructure.

TABLE I: Amazon's Kuiper Constellation Parameters

Altitude	Inclination	Planes	Sats/Plane	Satellites
630 km	51.9 deg	34	34	1156
610 km	42 deg	36	36	1296
590 km	33 deg	28	28	784

The higher shell of the Kuiper constellation was simulated on AGI's Systems Toolkit (STK) software. Table II provides the specific details of the evaluated scenario. The transmitter's beamwidth, EIRP and the receiver's antenna gain-to-noise-temperature (G/T) can be found in the documentation attached to the FCC application [13]. Three references points $N1$, $N2$ and $N3$ were deployed on the center, mid-range and far-range of one of the passing by satellite's footprint (see Figure 2), within the boundaries of initial service coverage latitudes [13]. To this end, a single satellite of the constellation was selected to evaluate the access over these ground points. The evolution of the Doppler frequency shift (see Figure 3) and C/N_0 values experienced by users at these points of interest were exported for two adjacent frequency channels along the satellite pass.

TABLE II: STK Scenario Parameters

Parameter	Value
Pass date	Jan 2020 00:03:00.0000
Tx Beamwidth	48.2 deg
Tx Frequency	19.298 GHz and 19.295 GHz
Tx EIRP	43.1 dBW
Rx G/T	14.1 dB/K
Modulation	BPSK
Data Rate	50 b/sec
CDMA spread	20460 chips/bit
Bandwidth	2.046 MHz
Atmospheric impairments	Cloud and fog (ITU-R P840-6) Tropo. scintillation (ITU-R P618-12) Ionospheric fading (ITU-R P531-13)

B. PNT Signals Generation

The Doppler profiles extracted from the simulated satellite passing over the three reference positions and the average C/N_0 levels were used to shape the GNSS-like signals generated by a digital signal generator. To this purpose, a GNSS signal generator named N-FUELS (FUll Educational Library of Signals for Navigation) [17] and based on MATLAB ® was employed. N-FUELS outputs digital baseband signals, simulating the behaviour of a user-defined RF front-end. It has been fed with the Doppler profiles sampled at 1 Hz.

The generated signals are BPSK-modulated with a chiprate of 1.023 MHz, often referred to as BPSK(1) in GNSS literature [18]. The purpose of using simple GNSS signals like the GPS L1 C/A signal [19] is twofold. On the one hand, we want to use a plain GNSS signal that does not add additional complexity to the receiver architecture. In this way we can steer the analysis to the tracking in LEO high-dynamics conditions and to the benefits of our proposed VWB architecture. On the other hand, since we are considering a fused secondary service on a broadband satellite payload, we want to limit the bandwidth resources devoted to PNT.

According to the documentation attached to the FCC application [13], Amazon Kuiper services will be delivered in the K_u,K and K_a bands. Supposing to host a PNT service on *user downlink beams*, the highest spectrum designation band during initial service deployment is a 500 MHz aggregated channel in the 18.8-19.3 GHz band. We chose to set the signal central frequencies in the highest available band in order to address

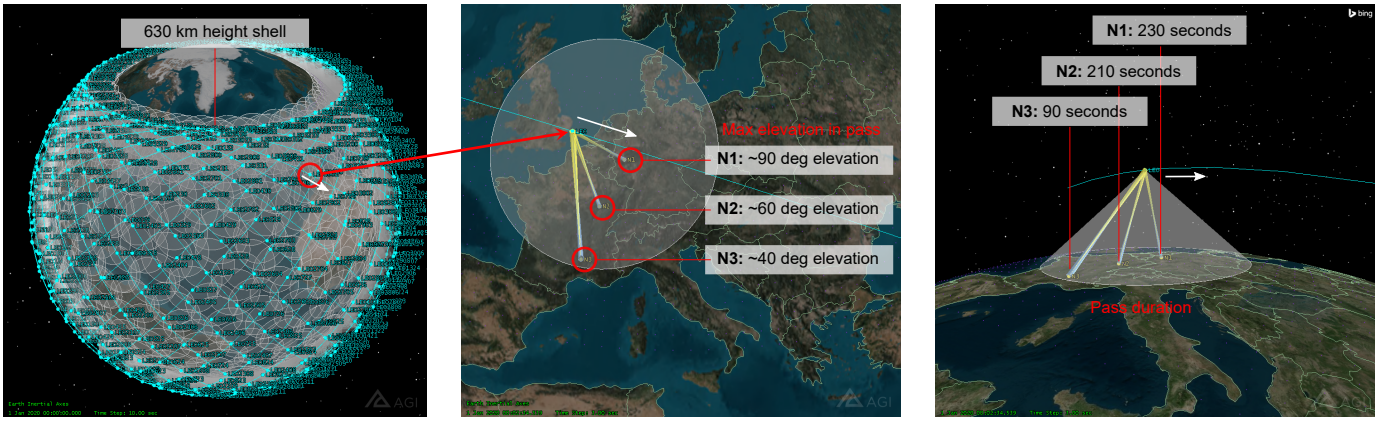

Fig. 2: Kuiper constellation and sample pass with reference points N1, N2 and N3.

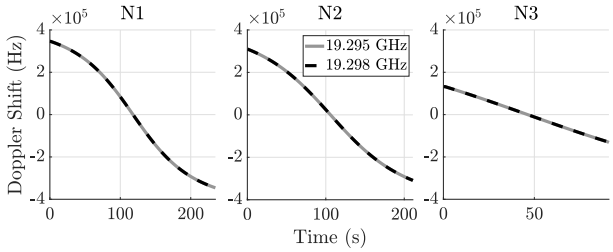

Fig. 3: Doppler profiles at reference points N1, N2 and N3.

TABLE III: Binary Signal Generator Parameters

Parameter	Value		
Sampling Frequency	25 MHz		
Intermediate Frequency	0 Hz		
Binary signal type	int8		
Quantization bits	7		
Code delay	0.5 ms		
Noise Density	-242.70 dBW-Hz		
-	**N1**	**N2**	**N3**
Average C/N_0 (dB-Hz)	107.71	106.90	104.83
Average Carrier power (dBW)	-134.98	-135.80	-137.87

a worst-case Doppler situation. Moreover, this condition will be also the most favorable for PNT from a theoretical point of view, since a higher carrier frequency has the potential to increase the estimation resolution [16].

Two PNT channels are necessary to build a meta-signal in the VWB receiver. To this end, we investigated the combination of one data channel and one pilot channel in two different arrangements, both commonplace in GNSSs signal plans:

S1 two BPSK(1) channels over the same bandwidth at a central frequency $f_c = 19.298$ GHz. Channels' multiple access is provided through orthogonality of spreading codes. This arrangement is similar to E1B and E1C in Galileo [20]

S2 two BPSK(1) channels on adjacent bands, centered at respectively f_c and $f_c' = 19.295$ GHz to accommodate a guard band in between.

The generation of the raw binary signals in N-FUELS is carried out according to the parameters in Table III, using constant C/N_0 levels based on the average values. The Doppler profiles (Fig. 3) obtained simulating the transmission of signals S1 and S2 in STK are loaded into the signal generator, which, after interpolation, apply them both on the carrier and on the spreading code. The net result is a set of realistic signals, that take into account the effect of Line-of-Sight (LOS) dynamics, the atmospheric effects (see Table II) and the presence of thermal noise at the receiver.

C. Receiver Processing Architecture

The binary signals have been processed through a GNSS software receiver based on MATLAB ®, which has been fine-tuned to properly track the LEO PNT signals of the Kuiper constellation. The configuration parameters are summarized in Table IV.

TABLE IV: Software Receiver Configuration

Parameter	Value
Coherent integration time	2 ms
PLL order	3
E-L spacing	1 chip
MSP E-L spacing	0.025 chip
Tracking Lock Indicator threshold	0.8
Virtual frequency separation	18 MHz

To properly track the LOS dynamics of the LEO context, a third order PLL has been used. It is worth noting that these kind of signals demand also a large PLL noise bandwidth and a large DLL noise bandwidth as well, if the latter is not taking advantage of a carrier aiding technique. The tracking loop is therefore generally less robust to thermal noise. However, the signals are also characterized by a C/N_0, which is much larger than commonplace GNSS values (around 45 dB-Hz [21]) and can counterbalance this drawback.

The tracking stage of the software receiver is a working VWB implementation of the open-loop block scheme originally presented in [11]. As described in Section II, the actual

MSP stage is triggered once the tracking loop is locked. A tracking lock indicator (PLI) as found in [22] is exploited to start the MSP stage once the PLI value is above the threshold defined in Table IV. The PLI is defined as

$$PLI = \frac{I_P^2 - Q_P^2}{I_P^2 + Q_P^2} \tag{3}$$

where I_P and Q_P are respectively the in-phase and quadrature P correlator outputs, computed at each tracking loop iteration.

Once the the MSP tracking loop is running, the E-L spacing is reduced to allow the DLL to take advantage of the enhanced gap between the P correlator and E or L correlator output (a consequence of the ACF peak sharpening). In order to get a fair comparison between single-channel processing and MSP, the nominal gap is left unaltered before and after the MSP triggering. The gap has been computed theoretically by considering the C/N_0 and the nominal ACFs of both the single BPSK(1) signal and the meta-signal (see Figure 1), A spacing of 0.25 chip has been therefore calculated as corresponding to the original spacing of 1 chip.

IV. Results

In this section we present and discuss the processing results provided by the MSP software receiver after tracking realistic LEO PNT signals. The main performance metric is the *code-rate error*, which has been estimated exploiting a noiseless signal. Such an ideal signal has been generated with identical characteristics and carrier power of the signal under test, but in the absence of thermal noise. The code-rate estimation is subject to LOS dynamic stress since the code tracking loop is not smoothed by carrier aiding. Each code-rate estimation is thus still affected by the code Doppler, which has not been smoothed. The estimated code-rate of the noiseless signal is characterized by the code Doppler as well and it can be successfully used to de-trend the S1 and S2 code-rate estimations. The code-rate error is then computed by subtracting the estimated code-rate of the noiseless signal to the estimated code-rate of the signal under investigation. The net result is a measure of the estimation error caused by the presence of thermal noise within the signals.

The estimated code-rate errors in Figure 4 were obtained from the six combinations of reference locations and signal arrangements. The Root Mean Square Errors (RMSEs) were extracted from the data in Figure 4 and reported in Table V as a comprehensive evaluation metric. RMSEs are computed separately over the initial single-channel stage (prior to MSP triggering) and the actual MSP stage, which begins after the tracking is considered locked (as indicated by the cyan vertical line). The RMSE of the single-channel stage is calculated by omitting the initial transient of the receiver's tracking loop, which is never below 0.05 s, as estimated by comparison with the noiseless processing outcomes. Nevertheless, the tracking lock indicator has been activated only after 5 s, to provide a meaningful statistic for single-channel RMSE.

It is worth noting that in all the plots in Figure 4 the S2 signal configuration performs better than S1. This is also

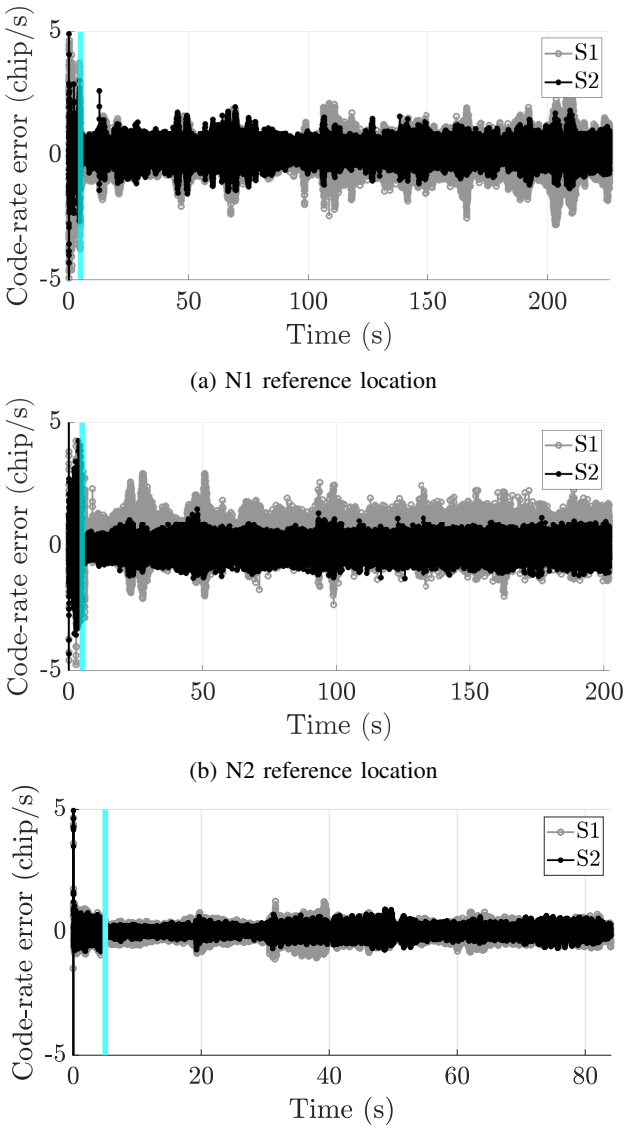

(a) N1 reference location

(b) N2 reference location

(c) N3 reference location

Fig. 4: Code-rate error for N1, N2 and N3 reference locations. The cyan line highlights the transition from single-channel processing to MSP.

TABLE V: RMSE of Code-Rate Estimations

-	N1		N2		N3	
-	***S1***	***S2***	***S1***	***S2***	***S1***	***S2***
Single-channel (chip/s)	1.96	1.68	1.44	1.29	0.34	0.29
MSP (chip/s)	0.51	0.37	0.61	0.30	0.23	0.19
RMSE reduction (%)	74.1	78.2	57.9	77.1	31.9	35.1

confirmed by Table V, where the RMSEs of S2 signals are always lower than those of S1. The two channels in the S2 configuration are centered over adjacent but different carriers. They experience therefore a different Doppler shift. These two channels, jointly processed within the MSP receiver, are thus characterized by different frequencies. Although this

difference is small (see Figure 3), this is in principle a challenging condition for the tracking loop. The PLL loops within the MSP architecture must be in fact sufficiently independent to successfully track different carriers. Nevertheless, the superimposed channels in S1 occupy the same bandwidth and they are potentially subject to a more correlated noise realization. The effect of this flaw exceeds probably the small impairment caused on S2 by the slightly different Doppler shifts, producing the outcomes in Figure 4 and Table V, where S2 is consistently confirmed the best-performing arrangement. Nonetheless, the performance of S1 and S2 are quite similar, meaning that through the VWB architecture it is possible to obtain almost the same code tracking performance of a signal (S2) which needs a bandwidth occupation which is at least doubled.

Figure 4a shows the code-rate error experienced in N1. This is the most challenging reference location because of the high Doppler effect experienced when the satellite passes over. The high-dynamics condition challenges the receiver and in fact the RMSE is generally higher at this reference location. However a substantial reduction of the estimation error is observable when MSP is employed, providing an improvement that is above 70% for both signal configurations (Table V). The intermediate elevation and Doppler levels experienced at location N2 result in a generally lower RMSE. But it is possible to see again a large reduction of RMSE thanks to MSP, confirming that in such conditions the technique is profitable and it can mitigate LOS dynamic stress. On the other hand, the MSP architecture becomes less beneficial when the Doppler effect intensity is limited, as in location N3. This is not the general case since MSP has been already applied in GNSS, at lower Doppler shifts [11]. However, under such favorable C/N_0 conditions (see Table III) it becomes more difficult to overtake the performance of a standard single-channel tracking loop.

V. Conclusions

In this paper we investigated the use of MSP applied to LEO PNT signals. We simulated a fused PNT service hosted by Amazon Kuiper, the forthcoming broadband mega-constellation. Realistic signals as received in three different Earth locations were processed according to a VWB paradigm for meta-signals. For a receiver that can bear the increased complexity of the implementation, the meta-signal architecture was proven an advantageous tracking scheme under high C/N_0 and large Doppler shifts, both peculiar conditions of LEO transmissions. The technique is especially effective at high Doppler levels. In fact, under such a favorable C/N_0 the benefits of the technique becomes less advantageous as we are approaching the limits of a noiseless receiver estimation processing. The high signal to noise ratio allows also to use large PLL and DLL noise bandwidths, hence adapting the software receiver to the high Doppler stress. However, a future analysis shall involve specific high-dynamics receivers, to further exploit the potential of a MSP architecture.

References

[1] European GNSS Agency, "GNSS market report issue 6," *European GNSS Agency: Luxembourg*, 2019.

[2] P. Teunissen and O. Montenbruck, *Springer handbook of global navigation satellite systems*. Springer, 2017.

[3] T. G. R. Reid, B. Chan, A. Goel, K. Gunning, B. Manning, J. Martin, A. Neish, A. Perkins, and P. Tarantino, "Satellite navigation for the age of autonomy," in *2020 IEEE/ION Position, Location and Navigation Symposium (PLANS)*, 2020, pp. 342–352.

[4] T. G. Reid, A. M. Neish, T. F. Walter, and P. K. Enge, "Leveraging commercial broadband leo constellations for navigation," in *Proceedings of the ION GNSS*, 2016, pp. 2300–2314.

[5] T. G. Reid, A. M. Neish, T. Walter, and P. K. Enge, "Broadband leo constellations for navigation," *NAVIGATION*, vol. 65, no. 2, pp. 205–220, 2018. [Online]. Available: https://onlinelibrary.wiley.com/doi/abs/10.1002/navi.234

[6] G. Gutt, D. Lawrence, S. Cobb, and M. O'Connor, "Recent PNT improvements and test results based on low earth orbit satellites," in *Proceedings of the 2018 International Technical Meeting of The Institute of Navigation*, 2018, pp. 570–577.

[7] P. A. Iannucci and T. E. Humphreys, "Economical fused LEO GNSS," in *2020 IEEE/ION Position, Location and Navigation Symposium (PLANS)*, 2020, pp. 426–443.

[8] J.-L. Issler, M. Paonni, and B. Eissfeller, "Toward centimetric positioning thanks to L-and S-band gnss and to meta-GNSS signals," in *2010 5th ESA Workshop on Satellite Navigation Technologies and European Workshop on GNSS Signals and Signal Processing (NAVITEC)*. IEEE, 2010, pp. 1–8.

[9] M. Paonni, J. Curran, M. Bavaro, and J. Fortuny, "GNSS meta-signals: coherently composite processing of multiple gnss signals," in *Proceedings of the 27th International Technical Meeting of The Satellite Division of the Institute of Navigation, Tampa, FL, USA*, 2014, pp. 8–12.

[10] P. Das, L. Ortega, J. Vilà-Valls, F. Vincent, E. Chaumette, and L. Davain, "Performance limits of GNSS code-based precise positioning: GPS, Galileo & meta-signals," *Sensors*, vol. 20, no. 8, 2020. [Online]. Available: https://www.mdpi.com/1424-8220/20/8/2196

[11] A. Nardin, F. Dovis, and B. Motella, "Impact of non-idealities on GNSS meta-signals processing," in *Proceedings European Navigation Conference (ENC) 2020*, Dresden, Nov. 2020.

[12] C. Henry, "Amazon's kuiper constellation gets FCC approval," *Space News*, 2020, Accessed on: Sep. 11, 2020. [Online]. Available: https://spacenews.com/amazons-kuiper-constellation-gets-fcc-approval

[13] Amazon, "Application of kuiper systems LLC for authority to launch and operate a non-geostationary satellite orbit system in Ka-band frequencies and attachments," 2019.

[14] J. W. Betz, "The offset carrier modulation for GPS modernization," in *Proceedings of the 1999 National Technical Meeting of The Institute of Navigation*, San Diego, CA, 1999, pp. 639–648.

[15] E. Kaplan and C. Hegarty, *Understanding GPS: principles and applications*. Artech house, 2005.

[16] W. C. Lindsey and M. K. Simon, *Telecommunication systems engineering*. Courier Corporation, 1991.

[17] E. Falletti, D. Margaria, M. Nicola, G. Povero, and M. T. Gamba, "N-FUELS and SOPRANO: Educational tools for simulation, analysis and processing of satellite navigation signals," in *2013 IEEE Frontiers in Education Conference (FIE)*, 2013, pp. 303–308.

[18] J.-A. Avila-Rodriguez, "On generalized signal waveforms for satellite navigation," *University FAF Munich, Munich*, 2008.

[19] U.S. Air Force, "NAVSTAR GPS space segment/navigation user segment interfaces (IS-GPS-200)," 2020.

[20] European Union, "Galileo open service, signal in space interface control document (OS SIS ICD V1.3)," 2016.

[21] A. Joseph and M. Petovello, "Measuring GNSS signal strength," *Inside GNSS*, vol. 5, no. 8, pp. 20–25, 2010.

[22] J. J. Spilker Jr, P. Axelrad, B. W. Parkinson, and P. Enge, *Global Positioning System: Theory and Applications, Volume I*. American Institute of Aeronautics and Astronautics, 1996.